

Supporting Information

Highly Electrocatalytic, Durable, and Stretchable Nanohybrid Fiber for On-body Sweat Glucose Detection

Phan Tan Toi^{†±}, Tran Quang Trung^{†±}, Thi My Linh Dang[±], Chan Wool Bae[±], and Nae-Eung
Lee^{±Δ[†]*}

[±]School of Advanced Materials Science & Engineering, Sungkyunkwan University, Suwon,
Kyunggi-do 16419, Korea

^ΔSKKU Advanced Institute of Nanotechnology, Sungkyunkwan University, Suwon, Kyunggi-
do 16419, Korea

[†]Samsung Advanced Institute for Health Sciences & Technology, Sungkyunkwan University,
Suwon, Kyunggi-do 16419, Korea

Email: nelee@skku.edu

[†] These authors contributed equally to this work

Supporting Figure S1

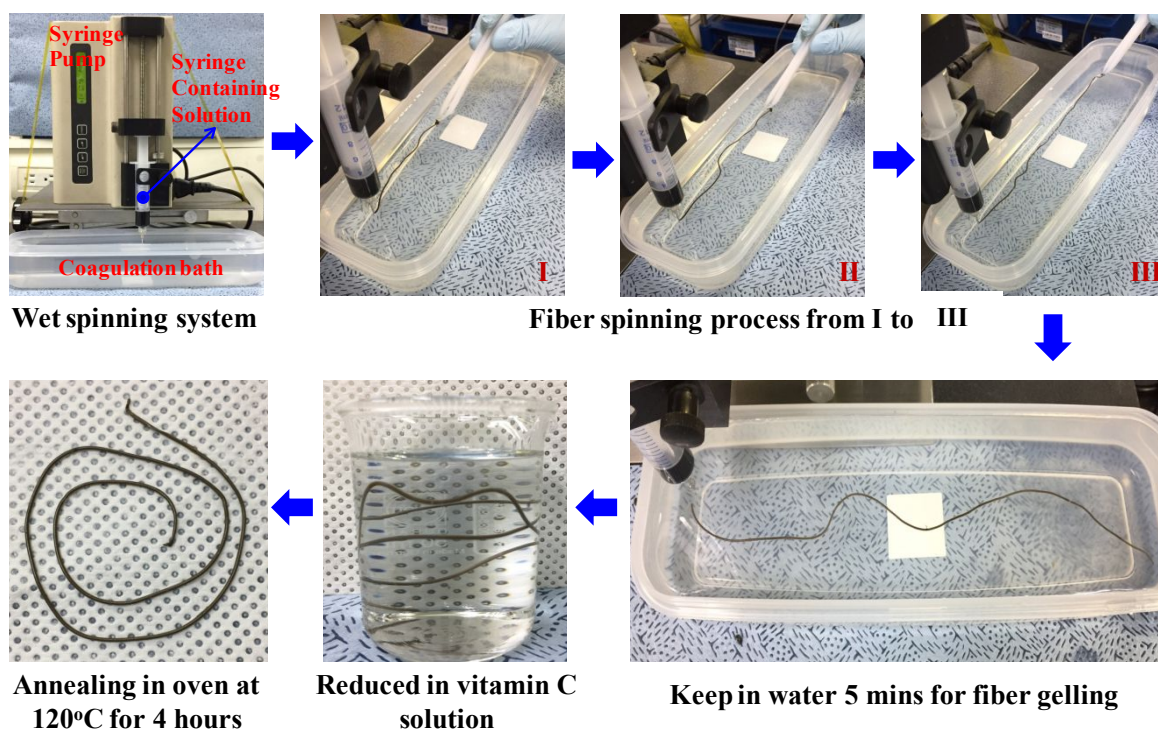


Figure S1: Optical images of the wet spinning system and fabrication process for the rGO/PU nanocomposite fiber.

To make the GO/PU fibers, we prepared various GO/PU solutions with different loading amounts of GO: 1.5 wt%, 2.5 wt%, 3.5 wt%, and 4.5 wt%. The GO/PU solutions with 1.5 wt% and 2.5 wt% of GO could not produce GO/PU fibers in a cylindrical shape because of the low incorporation of GO into the fiber. When we increased the loading amount of GO to 3.5 wt%, the fiber formed in a cylindrical shape. However, if we further increased it to 4.5 wt%, aggregation appeared in the solution, and we could not produce fibers. Therefore, we chose the GO/PU solution with 3.5 wt% of GO as the optimized condition for making GO/PU fiber.

Supporting Figure S2

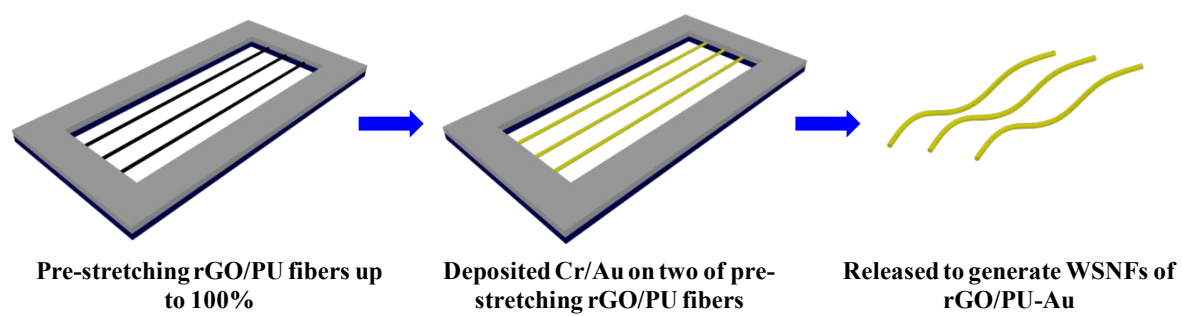


Figure S2: Schematic diagram of the fabrication process for WSNFs of rGO/PU-Au.

Supporting Figure S3

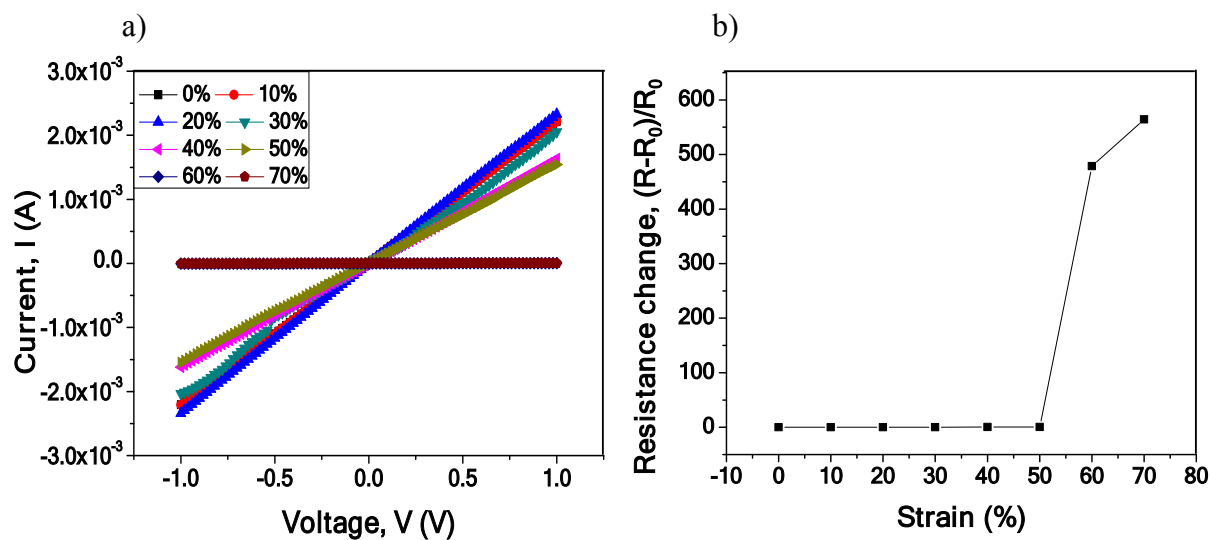


Figure S3: (a) I-V curves of WSNF under applied strain from 0 to 70%. (b) Resistance change of WSNF under applied strain from 0 to 70%.

Supporting Figure S4

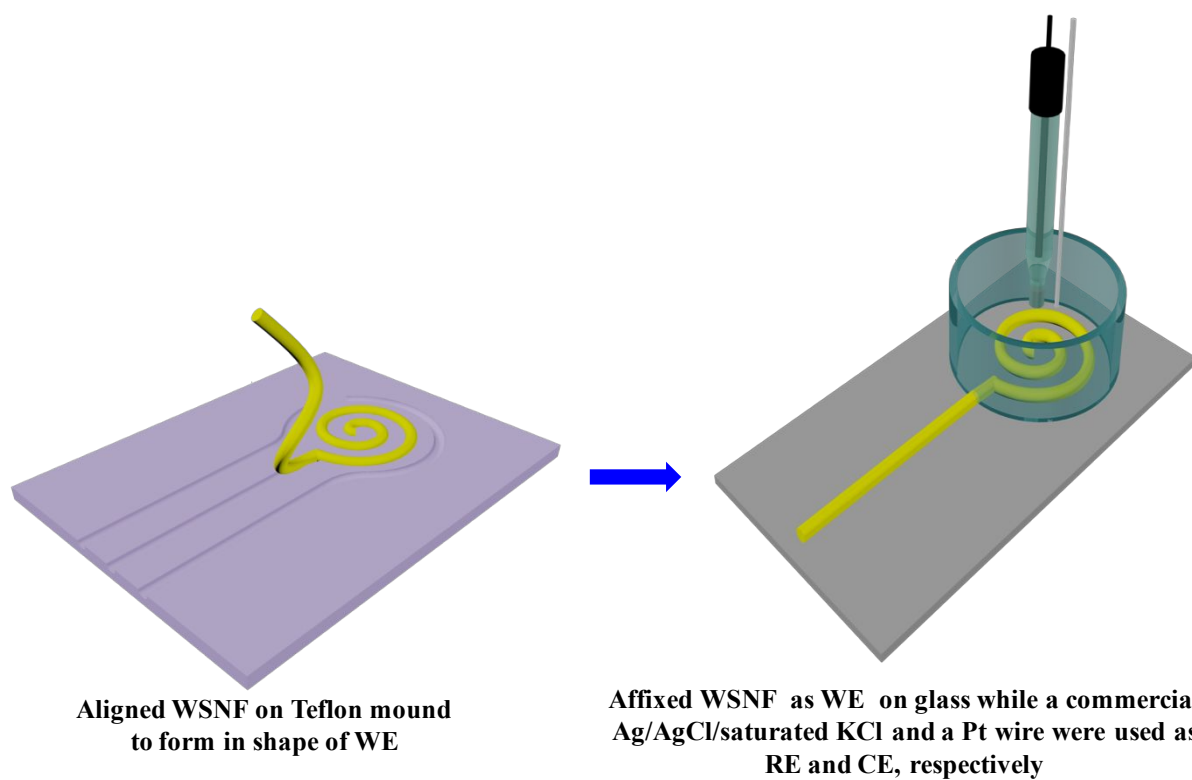


Figure S4: Schematic diagram presenting the fabrication and measurement set-up for fundamental characterization of the electrochemical glucose sensor using WSNFs as the WE and a commercial Ag/AgCl/saturated KCl and Pt wire as the RE and CE, respectively.

Supporting Figure S5

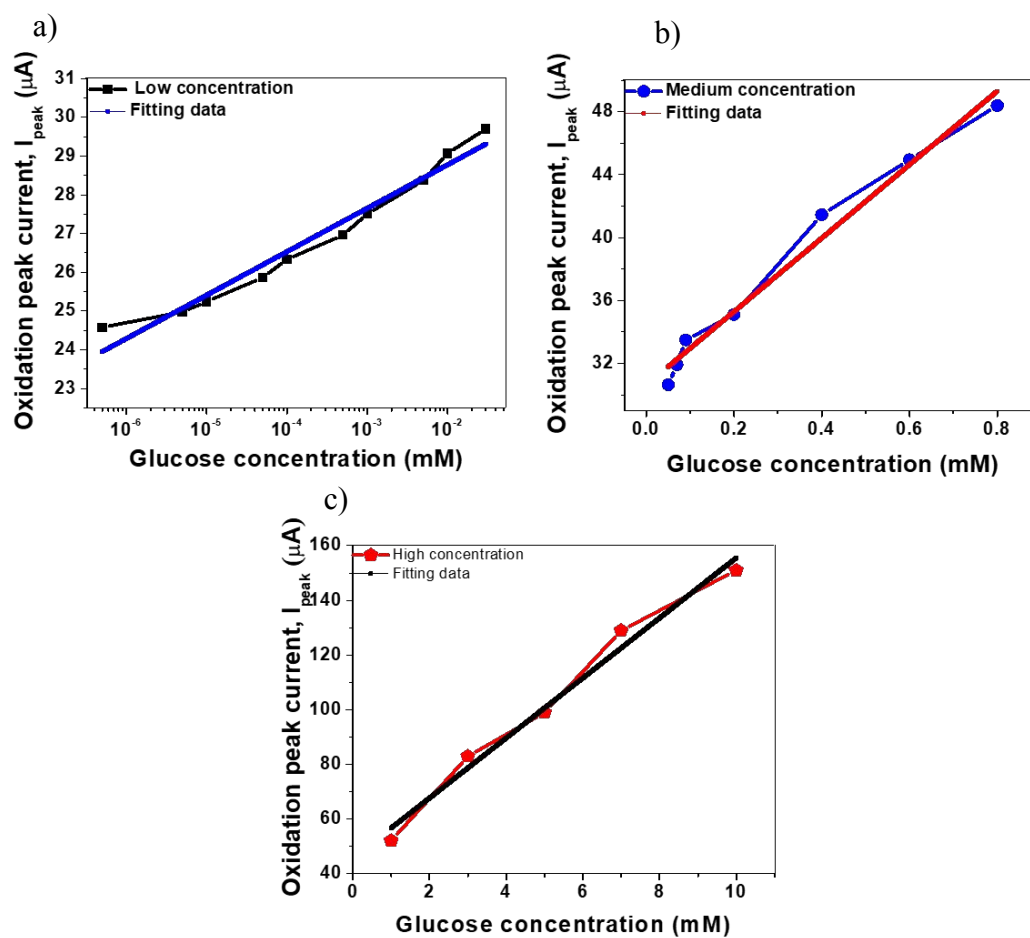


Figure S5: The I_{peak} of the WSNF electrode in the (a) low glucose concentration range, (b) medium glucose concentration range, and (c) high glucose concentration range.

Supporting Figure S6

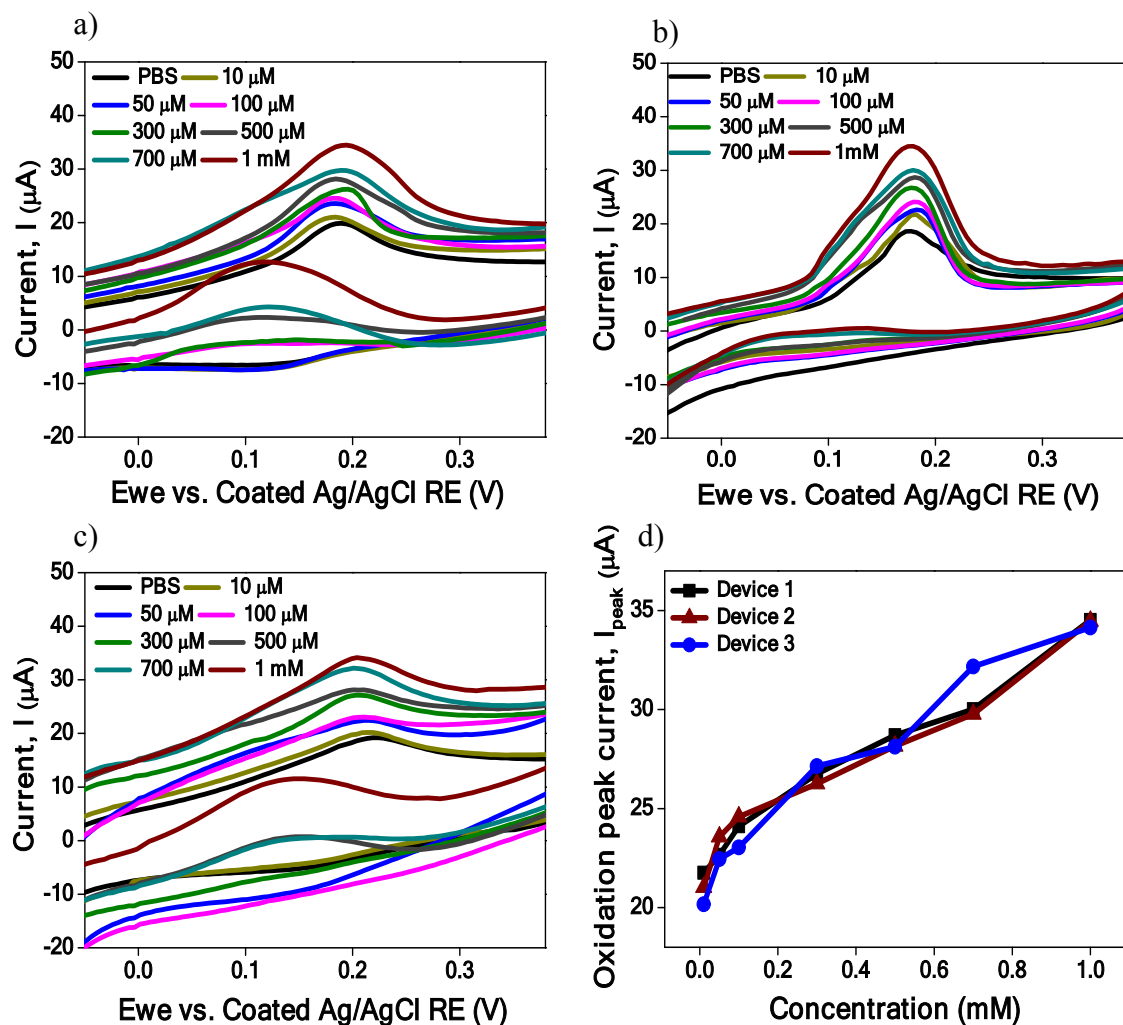


Figure S6: CV curves of three WSNF glucose sensors with the same fabrication conditions for (a) device 1, (b) device 2 and (c) device 3. (d) I_{peak} values as a function of glucose concentration.

Supporting Figure S7

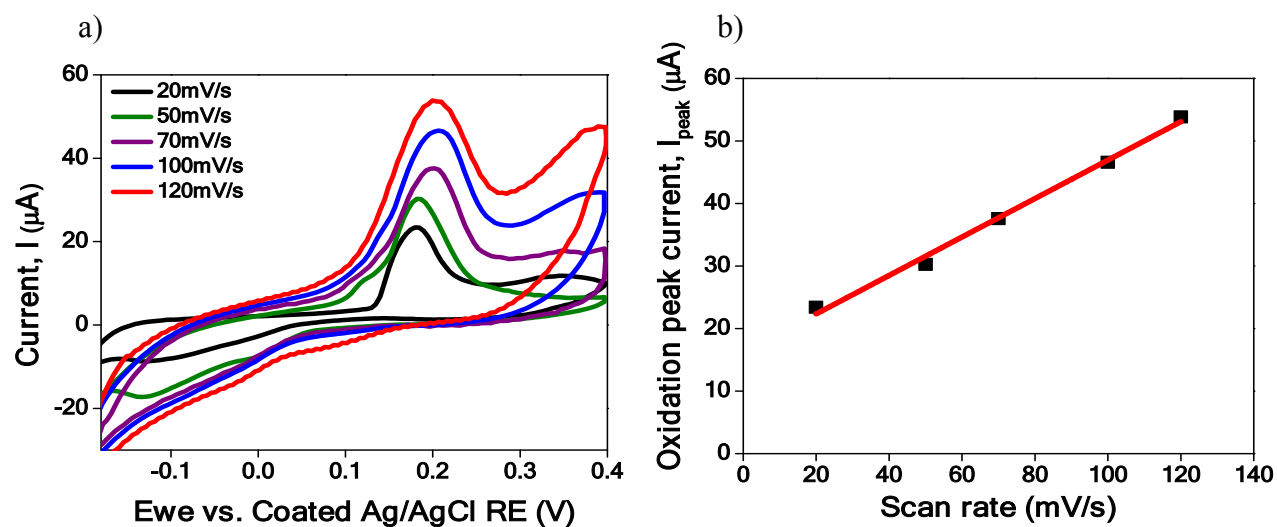


Figure S7: (a) CV curves of WSNF glucose sensor at various scan rates. (b) I_{peak} values as a linear function of the scan rate.

Supporting Figure S8

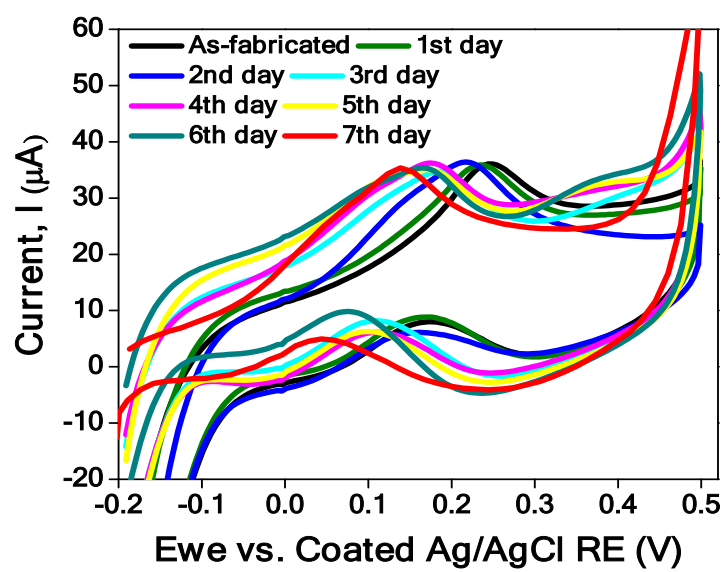


Figure S8: CV curves of the WSNF glucose sensor in 1 mM glucose solution after storage at ambient conditions for 7 days.

Supporting Figure S9

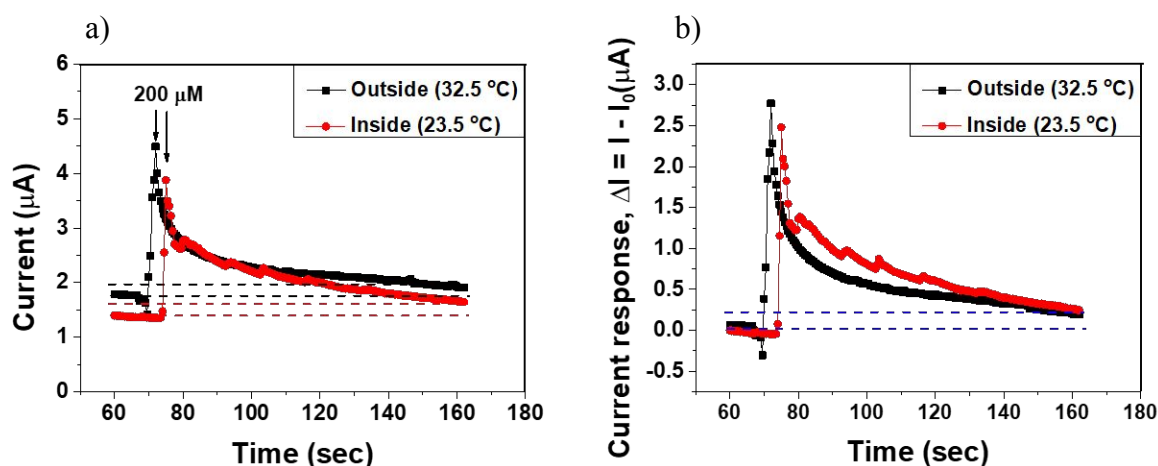


Figure S9: (a) CA current signals of the WSNF glucose sensor response to artificial sweat with 200 μM glucose concentration at outside and inside temperature. (b) Replotted response current (ΔI) of the WSNF glucose sensor at artificial sweat with 200 μM glucose concentration at outside and inside temperature.

Figure S9 presents the CA plot of WSNF glucose sensor response to artificial sweat contains 200 μM glucose which was measured at inside temperature (23.5 °C) and outside temperature (32.5 °C). We can see that the baseline current of the CA curves increased as the temperature increased from inside to outside (**Figure S9a**), possibly caused by the resistance change of the WSNF itself under temperature variation because of the thermal sensitivity of rGO in the WSNF sensor. However, the response current of the device, $\Delta I = I - I_0$, remained nearly unchanged at different temperatures (**Figure S9b**). These results demonstrate that the environment temperature does not contribute significantly to the glucose reaction but the resistance of the fiber decreased as the temperature increased due to the presence of rGO. To overcome this issue, the WSNF glucose sensor was also integrated with a stretchable temperature sensor. And the temperature sensor monitoring the temperature changes was used to correct the temperature-dependent glucose responsivity.

Supporting Figure S10

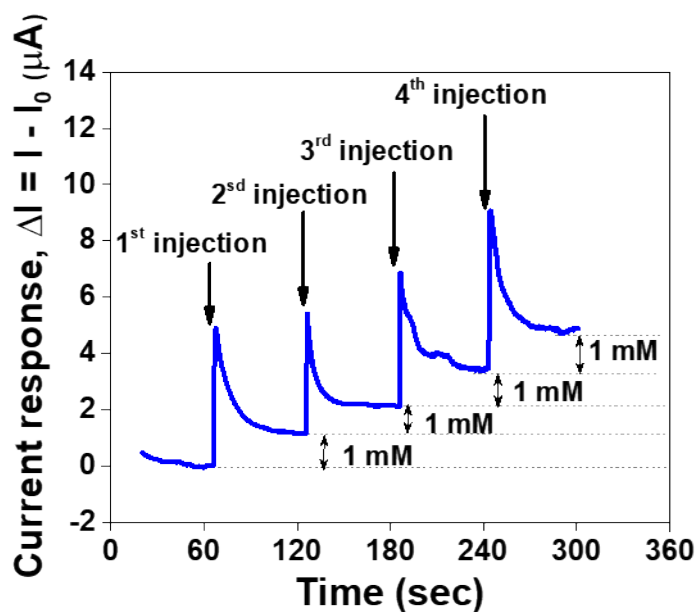


Figure S10: The CA response of stretchable WSNF glucose sensor by injecting the glucose solutions with the same concentration four times at saturation stage.

Figure S10 presents the CA response of stretchable WSNF glucose sensor by injecting the glucose solutions with the same concentration four times at saturation stage. It should be noted that the glucose concentration in this measurement is calculated based on the concentration and volume of the added glucose with the concentration and volume of the contained solution in well. The 100 μl of phosphate buffer saline 1X (PBS, Corning) is filled to run the baseline. In the first injection, to add 1 mM glucose concentration, we injected 100 μl glucose with 2 mM and kept it saturated in 60 s. Similar, to add 1 mM glucose concentration in the second, third, and fourth injection, we injected 100 μl glucose with 4 mM, 100 μl glucose with 6 mM, and 100 μl glucose with 8 mM, respectively.

Supporting Figure 11

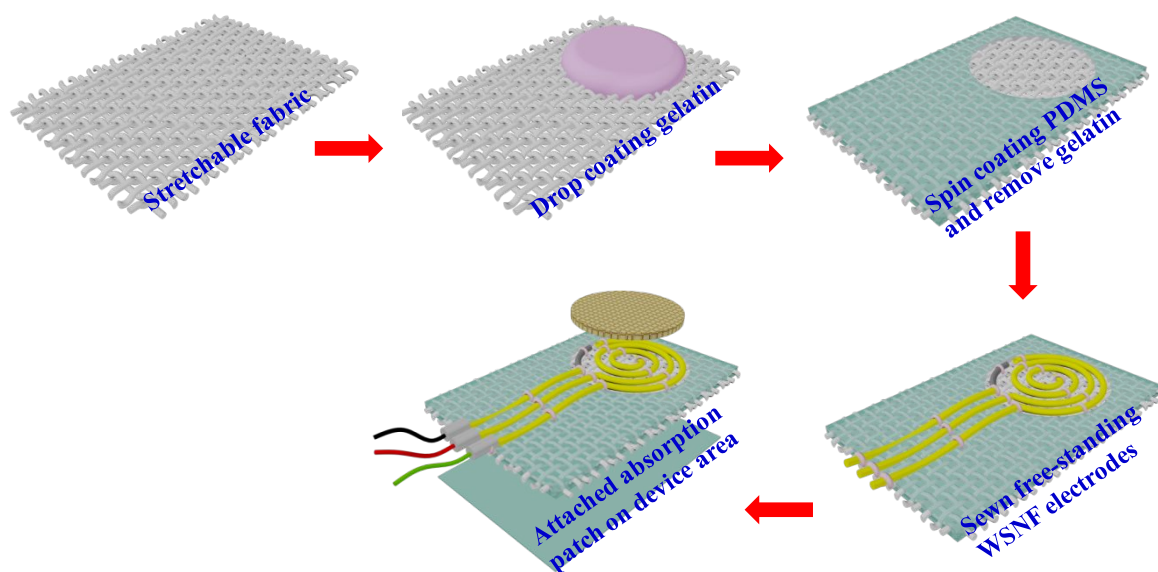


Figure S11: Schematic diagram presenting the fabrication process of the WSNF glucose sensor on stretchable fabric.

Supporting Table 1: Selected wearable glucose sensor in form factor of patch

Platform	Recognition element	Flexibility/stretchability	Methods	Sensitivity	Demonstration	Ref.
Polyethylene terephthalate	Glucose oxidase (Enzymatic)	Flexibility	Amperometric	-	On-human measurement	<u>1</u>
<u>Poly(dimethylsiloxane)</u>	Glucose oxidase (Enzymatic)	Stretchability (30 %)	Amperometric	-	On-human measurement	<u>2</u>
Polyimide	Glucose oxidase (Enzymatic)	Flexibility	Amperometric	130.4 $\mu\text{A}/\text{mM cm}^2$	On-human measurement	<u>3</u>
Stainless-steel	Nanoporous Pt (Non-enzymatic)	Flexibility	Amperometric	64.8 $\mu\text{A}/\text{mM cm}^2$	On-animal measurement	<u>4</u>
Wristband	Au rod (Non-enzymatic)	Flexibility	Amperometric	114 $\mu\text{A}/\text{mM cm}^2$	On-human measurement	<u>5</u>
<u>Poly(dimethylsiloxane)</u>	Au nanosheet (Non-enzymatic)	Stretchability (30 %)	Amperometric	10.89 $\mu\text{A}/\text{mM cm}^2$	On-human measurement	<u>6</u>
Elastomeric fiber	rGO/PU-Au nanohybrid wrinkled	Stretchability (30 %)	Amperometric	140 $\mu\text{A}/\text{mM cm}^2$	On-human measurement	This work

1. Gao, W.; Emaminejad, S.; Nyein, H. Y. Y.; Challa, S.; Chen, K.; Peck, A.; Fahad, H. M.; Ota, H.; Shiraki, H.; Kiriya, D.; Lien, D.-H.; Brooks, G. A.; Davis, R. W.; Javey, A., Fully integrated wearable sensor arrays for multiplexed in situ perspiration analysis. *Nature* **2016**, *529*, 509.

2. Lee, H.; Choi, T. K.; Lee, Y. B.; Cho, H. R.; Ghaffari, R.; Wang, L.; Choi, H. J.; Chung, T. D.; Lu, N.; Hyeon, T.; Choi, S. H.; Kim, D.-H., A *Graphene-Based Electrochemical Device with Thermoresponsive Microneedles for Diabetes Monitoring and Therapy*. *Nature Nanotechnol.* **2016**, *11*, 566.

3. Chen, Y.; Lu, S.; Zhang, S.; Li, Y.; Qu, Z.; Chen, Y.; Lu, B.; Wang, X.; Feng, X., *Skin-like biosensor system via electrochemical channels for noninvasive blood glucose monitoring. Sci. Adv.* **2017**, *3* (12), e1701629.
4. Yoon, H.; Xuan, X.; Jeong, S.; Park, J. Y., *Wearable, robust, non-enzymatic continuous glucose monitoring system and its in vivo investigation. Biosens. Bioelectron.* **2018**, *117*, 267-275.
5. Zhu, X.; Ju, Y.; Chen, J.; Liu, D.; Liu, H., *Nonenzymatic Wearable Sensor for Electrochemical Analysis of Perspiration Glucose. ACS Sens.* **2018**, *3* (6), 1135-1141.
6. Oh, S. Y.; Hong, S. Y.; Jeong, Y. R.; Yun, J.; Park, H.; Jin, S. W.; Lee, G.; Oh, J. H.; Lee, H.; Lee, S.-S.; Ha, J. S., *Skin-Attachable, Stretchable Electrochemical Sweat Sensor for Glucose and pH Detection. ACS Appl. Mater. Interfaces* **2018**, *10* (16), 13729-13740.